The Journal of Shimonoseki University of Fisheries 30 (1) 63 — 81 (1981)

Mössbauer Spectroscopic Study of Alkali Chloride Crystals Containing a Small Amount of Iron (II) *

By

Norihisa KAI

Contents

* Contribution from Shimonoseki University of Fisheries, No. 921. Received Aug.10, 1981.
This work is based on the author's thesis research in partial fulfilment of the requirements for the degree of Doctor at Department of Chemistry, Faculty of Science, Kyushu University.

Abstract

The behavior of a small amount of Fe^{2+} in the alkali chloride crystals was investigated mainly by the use of absorption Mössbauer spectroscopy. In cases of both lithium chloride and sodium chloride systems containing a small amount of iron (II), the single line absorption due to Fe^{2+} substituted for Li^+ or Na^+ was observed at room temperature. The assignment was also justified from the results obtained in Mössbauer spectrum measurements of both LiCl (^{57}Fe) and NaCl (^{57}Fe) systems containing about 0.1 atomic percent (abbreviated as at%) of enriched iron-57(II). ^{60}Co-γ ray irradiation experiments were also performed for the both systems to elucidate the interaction between Fe^{2+} and defects in the crystals, but irradiation effects were not observed.

In cases of potassium chloride and rubidium chloride systems containing a small amount of iron(II), only one doublet absorption with the isomer shift characteristic of ionic ferrous ion was observed at room temperature. Each doublet absorption was interpreted as to be arisen from the K_2FeCl_4 compound in case of potassium chloride system and the Rb_2FeCl_4 compound in case of rubidium chloride system, respectively. The assignment was also justified from the results obtained in X-ray diffraction and Mössbauer spectrum measurements of the potassium- and rubidium-chloroferrate compounds prepared in an electric furnace. ^{60}Co-γ ray irradiation effects were not observed for the potassium- and rubidium-chloroferrate compounds.

In case of cesium chloride system containing a small amount of iron (II), one doublet absorption with the isomer shift characteristic of ionic ferrous ion was observed only at liquid nitrogen temperature. The absorption was assigned to the Cs_3FeCl_5 compound from the results obtained in X-ray diffraction measurement of the cesium chloride system.

1. Introduction

When divalent metal impurity ions are incorporated into an alkali halide lattice, they go in substitutionally for alkali ions[1]. Because of the extra positive charge of these ions and the requirement of charge neutrality, an equal number of negatively charged defects must also be simultaneously introduced. In the light of this reason, the positive-ion vacancy is the most probable defect to be formed in pure alkali halide. As a result, in the absence of other chemical impurities, divalent cation addition will be accompanied by the introduction of an equal number of positive-ion vacancies[1]. This is illustrated in Fig. 1 (a) and (b).

Because controlled numbers of positive-ion vacancies can be introduced in this manner, alkali halides doped with divalent cations have been studied extensively in the past in order to determine the properties of the positive-ion vacancy[1].

However, a complete interpretation of these experiments has not been possible because the importance of interaction between the divalent cations and the vacancies has not been known. A positive-ion vacancy, being a missing positive

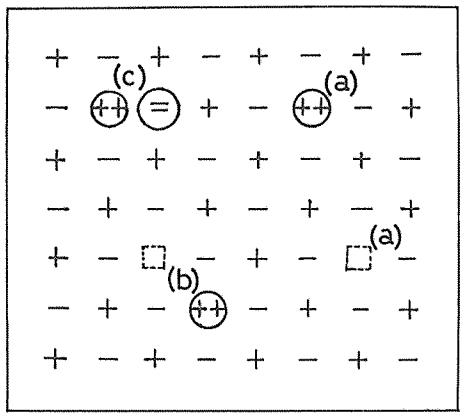

Fig. 1. Divalent ion incorporation in an alkali halide lattice. Charge compensation may arise from positive-ion vacancies either (a) separated, or (b) bound to the ion. Possible charge compensation by another chemical impurity is shown as (c).

charge, can be considered as carrying an effective negative charge in the lattice. It will experience a coulombic attraction to the extra positive charge of a divalent ion and may tend to pair off with it, as shown in Fig. 1 (b). This complex is called a simple associated pair. Complexes involving more than one defect are also possible. The pair of Fig. 1 (b) will usually contribute differently to the physical property being measured than the isolated defects of Fig. 1 (a). Therefore, in order to interpret the experiments properly, it is necessary to know the degree to which association occurs. Detailed understanding will also require knowledge of the types of complexes involved, and theoretical estimates have been made indicating that significant association should occur[2~4].

Experimental evidence of association has also been cited in ionic conductivity[1], dielectric loss[1], diffusion[1], optical coloration[5] and nuclear resonance[6] measurements on these or similar crystals. However, these methods give less detailed information than the electron spin resonance studies, because they are relatively indirect and may not lend themselves to unambiguous interpretation. But our understanding on the problem is still ambiguous because the published data are inconsistent with each other in some cases. Hence, an attempt to solve the ambiguous point has been done by means of Mössbauer spectroscopy. In the first place, the principle of Mössbauer effect is briefly described below.

The Mössbauer effect is the recoilless emission and resonant absorption of γ-rays. The resonant absorption is observed when the energy of γ-rays (14.4 keV) emitted from the excited nucleus is matched to the difference of the energy levels between the excited and ground states of the absorber (Fig. 2). Its importance lies in the production of extremely monochromatic radiation which can be used as a spectroscopic source of energy to probe details of chemical structure and bonding. The precise energy of the resonant transition is influenced by three hyperfine interactions.

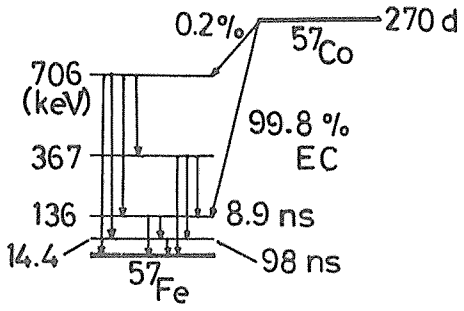

Fig. 2. Energy levels of Mössbauer (^{57}Fe) nucleus.

The first of these interactions gives rise to a chemical isomer shift, δ, and originates in the varying coulombic interaction between the positive nucleus of an atom and its electronic environment. The isomer shift is directly proportional both to the change in nuclear radius on excitation, $\delta R/R$, and to the change in s-electron density at the nucleus on going from the source to the absorber. Its magnitude is determined by the following factors:

1. Electronic configuration of the atom, including
   (a) oxidation state
   (b) spin multiplicity
2. Shielding effects of p, d and f electrons on the s-electron density at the nucleus
3. Covalency effects in modifying s, p and d electron population and distribution, including
   (a) σ withdrawal of electrons by electronegative groups
   (b) deshielding due to d_π back donation

The second hyperfine interaction from which information can be obtained is the quadrupole splitting, Δ. Any nuclear state with a spin quantum number $I > 1/2$ has a quadrupole moment, Q, which is able to interact with an electric field gradient, q, to lift the degeneracy of the state. In the simplest case of a transition between $|\pm 3/2>$ and $|\pm 1/2>$ in an axially symmetric electric field gradient, the quadrupole splitting, Δ, is directly proportional to both Q and q. In general, it has been found that Δ is an extremely powerful probe of local site symmetry and its magnitude has been found to depend on:

1. Electronic configuration of the atom, including
   (a) oxidation state
   (b) spin multiplicity
2. Site symmetry, including effect of
   (a) coordination number
   (b) cis-trans isomerism
   (c) ligand-field distortion etc.
3. Contributions from neighboring charges (atoms or ions)
   (a) asymmetric withdrawal of p and d electrons for bonding
   (b) polarizable atoms in covalent assemblies
   (c) lattice terms in ionic crystals

The third hyperfine interaction which influences the Mössbauer spectrum is the nuclear magnetic Zeeman splitting which arises when the nucleus is subject to an internal or an applied magnetic field. The extent of the energy separation depends both on the nuclear magnetic moments of the ground and excited states, and also on the magnitude of the magnetic field, H. Thus in ^{57}Fe the $|\pm 1/2>$ ground state splits into two sublevels and the $|\pm 3/2>$ excited state splits into four sublevels; transitions between these are normally subject to the selection rules of $m=0$ and 1 so that six resonance lines will be seen. If an electric field gradient is also present then there is a perturbation which disturbs the even spacing of lines and enables the mutual orientation of H and q to be determined.

From a general theory described above, we will be able to appreciate that Mössbauer spectroscopy is widely applied to the problems in solids[7~9]. The type of solids used for the study ranges from inorganic compounds to metals and alloys[9]. The way of using the Mössbauer spectroscopy is divided into two different categories, *i.e.*, emission Mössbauer spectroscopy and absorption Mössbauer spectroscopy. The emission Mössbauer spectroscopy consists of the source containing ^{57}Co in the sample and the absorber containing natural or enriched (^{57}Fe) iron nuclei. The

absorption Mössbauer spectroscopy is essentially the same with the emission Mössbauer spectroscopy except that the iron nuclei are in the sample and that the ^{57}Co nuclei are outside the sample.

Over the past seventeen years a great deal of effort has been invested in investigating the nature of defect association of dispersed divalent ions in an alkali halide host by employing emission Mössbauer spectroscopy[10~20]. Crystals doped with low concentrations of ^{57}Co, the radioactive parent atom of the stable Mössbauer isotope ^{57}Fe, have been used as sources. The spectral distribution of 14.4 keV γ-ray from these sources is analysed with a standard single line absorber such as potassium ferrocyanate in these source studies.

MULLEN[10] found the species present at high concentrations (10^4 ppm) to be essentially Fe^{2+} (presumably an aggregate), while at lower concentrations (10 ppm) the Fe^{2+} disappeared, and a doublet with an isomer shift corresponding to Fe^{3+}, and a single line with a negative isomer shift corresponding to Fe^{+} were seen[11]. The kinetics rather than thermodynamic stability of this system was emphasized by the increase in the intensity of the Fe^{+} peak if the crystal was quenched rapidly from high temperature; slow cooling gave Fe^{3+} only. Both KCl[16] and LiF[18] gave essentially similar spectra, with an Fe^{3+} doublet.

The origin of the Fe^{+} peak is not clear; it could arise either from Co^{+} or Co^{2+}, but the absence of quadrupole splitting would suggest that it is not associated with vacancies. Co^{+} may be produced by the electron capture decay of ^{57}Co nuclei, followed by the auto-radiolysis of the crystal. Even in the few hours required to accumulate a spectrum, the crystal will receive a considerable radiation dose (10^{17} eV/g in 10 hr, assuming 100 keV/decay), and in view of the effects of irradiation on the EPR spectra, this could be expected to change the initial state of the cobalt atoms. KAMAL and MENDIRATTA[15] found that further irradiation of the crystals with X-rays produced no further effects, implying that the dose from the ^{57}Co may have saturated the crystal.

In all cases the ^{57}Co was introduced in the +2 oxidation state, but a signal corresponding to Fe^{2+} was seen in only one case[12], where very low concentrations were used, and the crystals were annealed and cooled very carefully in the absence of light. HENNIG and Kim YUNG[12] claim that the large quadrupole splitting is due to another divalent negative impurity ion such as O^{2-} as shown in Fig. 1 (c), but it could equally be due to a nearby vacancy.

The only work on sodium fluoride[19] introduced the cobalt by diffusing a film of metal into the crystal; the resulting spectrum was very different from the results obtained for NaCl, and shows all the features of the high concentration Fe^{2+} region.

As described above, the results of these investigations have been brought with controversy. The conflicting spectra observed exhibit multiple charge states Fe^{+}, Fe^{2+} and Fe^{3+}. It is puzzling that a simple impurity-vacancy dipole model shown in Fig. 1 (b) has not found any support from source studies, while ESR experiments[21] on stable divalent ions in alkali halides have convincingly demonstrated the existence of such dipoles. A corresponding Mössbauer absorber study employing alkali halide crystals doped with stable ^{57}Fe isotopes has never been tried due to the need of using concentration of ^{57}Fe far in excess of its solubility limit. Further, somewhat difficult chemistry in the laboratory preparation of $^{57}FeX_2$ (X=F, Cl, Br, etc) in significant amounts

and its introduction into the alkali halide crystals in the dispersed form has tended to discourage absorber studies.

In the present study an attempt to elucidate the behavior of a small amount of Fe^{2+} in alkali chloride crystals was made mainly by the use of absorption Mössbauer spectroscopy.

2. Experimental

2·1 Materials

Alkali chloride crystals containing a few at% of iron(II) were prepared by melting a mixture of weighed quantities of alkali chloride and iron(II) chloride in N_2 atmosphere at 800°C for 2 hr in an electric furnace (Fig. 3). The melt was then quenched quickly by compressing it between two copper plates. Iron contents were determined to be about 3 at% in all the samples from an EDTA titration method.

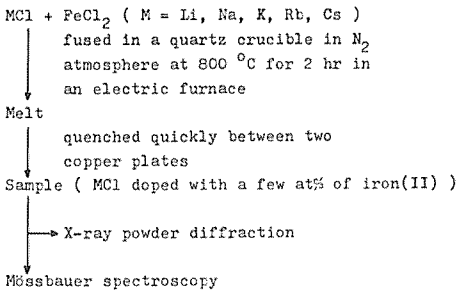

Fig. 3. Experimental scheme for MCl (Fe) system (M = Li, Na, K, Rb and Cs) containing a few at% of iron (II).

Lithium chloride and sodium chloride samples containing about 0.1 at% of enriched iron-57(II) were also prepared for comparison by using the electric furnace shown in Fig. 5. Iron-57(II) chloride used for the doping experiments was prepared in the same way as in the ref. 22 (Fig. 4).

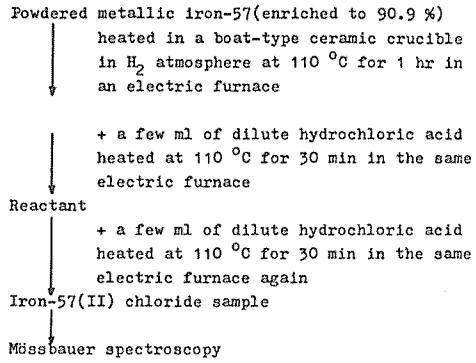

Fig. 4. Experimental scheme for the preparation of iron-57(II) chloride sample.

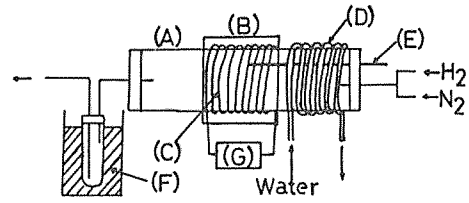

Fig. 5. Electric furnace used for the sample preparations: (A) Quartz tube; (B) Asbestos; (C) Kanthal coil; (D) Condenser; (E) Thermometer; (F) Dry ice; (G) Electric source.

From the Mössbauer spectra (Fig. 6) and parameters (Table 1) for the iron-57(II) chloride samples, the heated sample (b) containing anhydrous iron-57(II) chloride (absorption (III_{Fe})) was used for the doping experiments because the sample (a) contains a large amount of iron-57(II) chloride

tetrahydrate (absorption (II_{Fe})) which is easily decomposed to α-$^{57}Fe_2O_3$ below a melting temperature in doping experiments. A mixture of weighed quantities of dehydrated lithium chloride (or sodium chloride) and the iron-57(II) chloride was placed in a boat-type ceramic crucible and fused at 750°C (at 850°C in case of sodium chloride) for 5 min under N_2 atmosphere (Fig. 7). The melt was then quenched quickly by sliding the crucible under the condenser for cooling shown in Fig. 5.

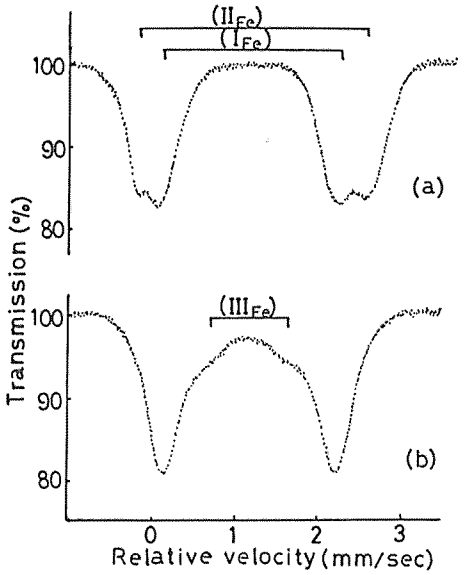

Fig. 6. Mössbauer spectra of iron-57 (II) chloride sample before (a) and after (b) the heat treatment at 200°C for 1 hr under H_2 atmosphere.

Table 1. Mössbauer parameters for iron-57(II) chloride sample before (a) and after (b) the heat treatment at 200°C for 1 hr under H_2 atmosphere. δ and Δ represent the isomer shift and quadrupole splitting values, respectively

(mm/sec)

Sample		δ (±0.01)	Δ (±0.02)
(a)	(I_{Fe})	1.17	2.31
	(II_{Fe})	1.20	3.06
(b)	(I_{Fe})	1.17	2.21
	(III_{Fe})	1.10	0.83

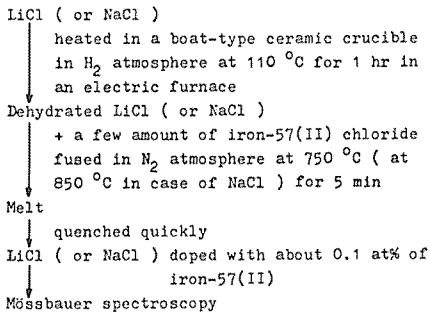

Fig. 7. Experimental scheme for LiCl (^{57}Fe) and NaCl (^{57}Fe) system containing about 0.1 at% of iron-57(II).

Potassium-chloroferrate compounds ($KFeCl_3$ and K_2FeCl_4)[23] shown in Fig. 8 were prepared for comparison by melting a mixture of weighed quantities of potassium chloride and hydrated ferrous chloride (K/Fe=1,2 and 3) at 500°C for 1 hr under N_2 atmosphere in the electric furnace shown in Fig. 5 (Fig. 9).

Rubidium-chloroferrate compounds ($RbFeCl_3$, Rb_2FeCl_4 and Rb_3FeCl_5)[24] shown in Fig. 10 were also prepared for comparison in the same way as in the case of potassium-chloroferrate compounds except that the temperature in an electric furnace was kept at 600 °C (Fig. 11). The dehydration of water molecules in chemical reagent $FeCl_2 \cdot 4H_2O$ was carried out before the fusion for both systems, at 300°C for 1 hr in the same electric furnace under H_2 atmosphere.

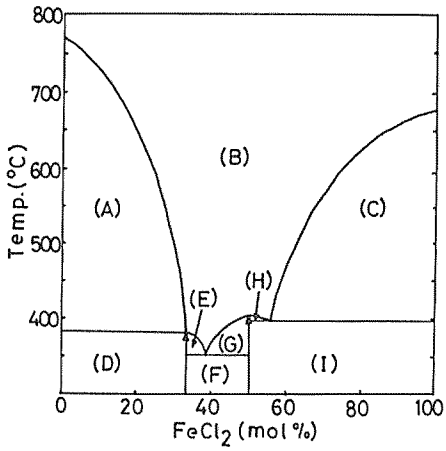

Fig. 8. Phase diagram of KCl-$FeCl_2$ system :
(A) Liq.+KCl,
(B) Liquid,
(C) Liq.+$FeCl_2$,
(D) KCl+K_2FeCl_4,
(E) Liq.+K_2FeCl_4,
(F) K_2FeCl_4+$KFeCl_3$,
(G), (H) Liq.+$KFeCl_3$,
(I) $KFeCl_3$+$FeCl_2$.

KCl + $FeCl_2 \cdot 4H_2O$ (K/Fe = 1, 2, 3)
↓ dehydrated in a quartz crucible in H_2 atmosphere at 300 °C for 1 hr in an electric furnace
↓ fused in N_2 atmosphere at 500 °C for 1 hr
Melt
↓ quenched quickly
Sample
↓
X-ray powder diffraction
Mössbauer spectroscopy

Fig. 9. Experimental scheme for the preparation of potassium-chloroferrate compounds.

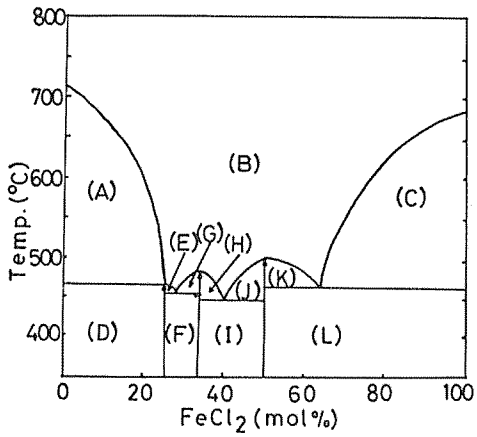

Fig. 10. Phase diagram of RbCl-$FeCl_2$ system :
(A) Liq.+RbCl,
(B) Liquid,
(C) Liq.+$FeCl_2$,
(D) RbCl + Rb_3FeCl_5,
(E) Liq.+Rb_3FeCl_5,
(F) Rb_3FeCl_5+Rb_2FeCl_4,
(G), (H) Liq.+Rb_2FeCl_4,
(I) Rb_2FeCl_4+$RbFeCl_3$,
(J), (K) Liq.+$RbFeCl_3$,
(L) $RbFeCl_3$+$FeCl_2$.

RbCl + $FeCl_2 \cdot 4H_2O$ (Rb/Fe = 1, 2, 3)
↓ dehydrated in a quartz crucible in H_2 atmosphere at 300 °C for 1 hr in an electric furnace
↓ fused in N_2 atmosphere at 600 °C for 1 hr
Melt
↓ cooled slowly
Sample
↓
X-ray powder diffraction
Mössbauer spectroscopy

Fig. 11. Experimental scheme for the preparation of rubidium-chloroferrate compounds.

2·2 Mössbauer spectroscopy

Mössbauer measurements were carried out with a conventional spectrometer operating in the time mode. Cobalt-57 (5 mCi) diffused into a palladium foil was used as a source. The velocity scale was calibrated with a metallic iron foil, which was also used as a reference for the isomer shift values. All spectra were fitted to a Lorenzian line shape using a least squares iteration procedure.

2·3 ^{60}Co-γ ray irradiation

Lithium chloride and sodium chloride samples containing about 0.1 at% of enriched iron-57(II) and potassium- and rubidium-chloroferrate compounds were irradiated with ^{60}Co-γ rays at room temperature at the ^{60}Co-γ rays irradiation facility of Kyushu University. All the samples were crushed and pulverized in an agate mortar in N_2 atmosphere and were placed in a polyethylene bag filled with N_2 gas. The γ-ray irradiation was performed in the range of 1×10^8 R$\sim$ 1×10^9 R with a dose rate of 1×10^6 R/hr.

2·4 The other measurements

X-ray powder diffraction measurements were carried out with nickel filtered Cu-Kα radiations, at Kyushu Environmental Evaluation Association.

3. Results and Discussion

3·1 LiCl-$FeCl_2$ and NaCl-$FeCl_2$ systems

In the Mössbauer spectrum for the LiCl(Fe) system containing a few at% of iron, only a single line with the isomer shift characteristic of ionic ferrous ion was observed at room temperature (Fig. 12 (a) and Table 2). It is noteworthy that the single line for the Fe^{2+} has rarely been observed so far.

In general, the quadrupole splitting for the ferrous ion in an octahedral environment will mainly be originated from the q_{val} value arisen from the non-cubic distribution of d-electrons in the Fe^{2+}. Hence, the interpretation for the single line is considered to be difficult. In a few other previous papers, the interpretation is inconsistent with each other[25, 26]. Mössbauer measurement for this system was then performed at both liquid nitrogen and helium temperatures, but no splitting of the single line was observed in

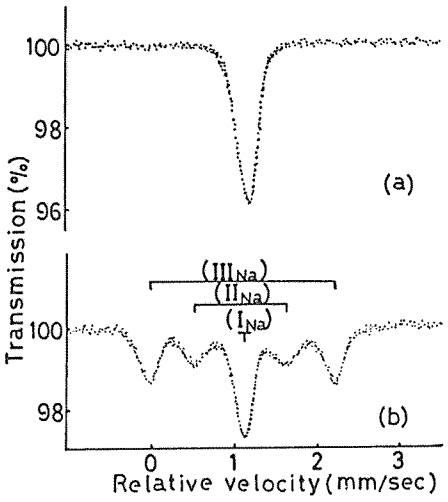

Fig. 12. Mössbauer spectra of (a) LiCl(Fe) system and (b) NaCl (Fe) system.

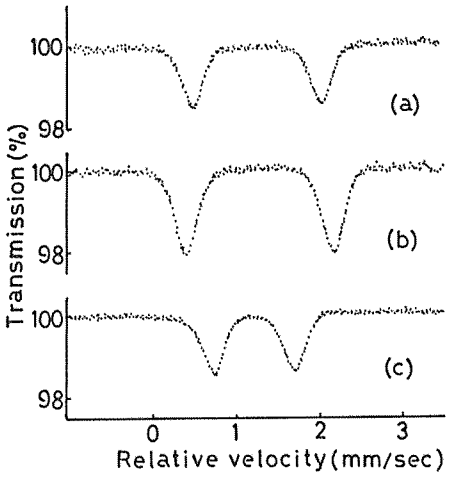

Fig. 13. Mössbauer spectra of (a) KCl (Fe) system, (b) RbCl (Fe) system and (c) CsCl (Fe)* system.

*at liq. N_2 temperature.

Table 2. Mössbauer parameters for each alkali chloride sample containing a few at% of iron. δ and Δ represent the isomer shift and quadrupole splitting values, respectively

(mm/sec)

Sample		δ (±0.01)	Δ (±0.02)
LiCl(Fe)		1.13	0
NaCl(Fe)	(I_{Na})	1.12	0
	(II_{Na})	1.09	1.01
	(III_{Na})	1.13	2.33
KCl(Fe)		1.12	1.57
RbCl(Fe)		1.18	1.74
CsCl(Fe)*		1.06	1.04

* measured at liq. N_2 temperature.

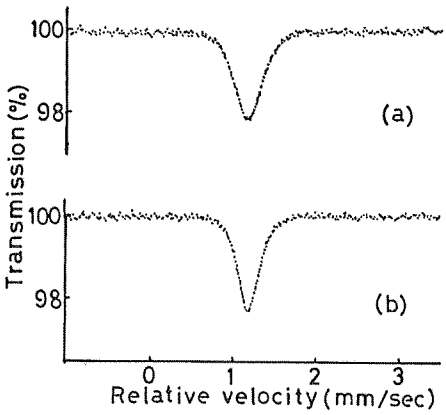

Fig. 14. Mössbauer spectra of (a) LiCl (^{57}Fe) system and (b) NaCl (^{57}Fe) system.

Table 3. Mössbauer parameters for lithium chloride and sodium chloride samples containing about 0.1 at% of iron-57(II). δ, Δ and Γ represent the values of isomer shift, quadrupole splitting and line width, respectively

(mm/sec)

Sample	Temp. (K)	δ (±0.01)	Δ (±0.02)	Γ (±0.02)
LiCl(^{57}Fe)	296	1.13	0	0.43
	78	1.25	0	0.45
NaCl(^{57}Fe)	296	1.15	0	0.31
	78	1.27	0	0.33

contrast with the result for the ^{57}Fe-doped CdF_2[27]. This single line is therefore interpreted as to be arisen from Fe^{2+} substituted for Li^+ located in the cubic site. This consideration is also justified from the fact that there was no change in the X-ray diffraction lines between the pure LiCl and the iron-doped LiCl, and that a melting point depression of the lithium chloride sample was observed in the differential thermal analysis. Since the Fe^{2+} can be considered to be located in a perfectly symmetric site, there will be slightly negative-charged vacancy in the nearest neighbor[28]. Mössbauer spectrum measurement for LiCl doped with about 0.1 at% of ^{57}Fe(II) was carried out for comparison at both room and liquid nitrogen temperatures (Fig. 14 (a)), but the Mössbauer spectral change was not observed as in the case of LiCl(Fe) system (Table 3). This shows that the spin-spin or spin-lattice relaxation time of a small amount of Fe^{2+} in lithium chloride crystal is very fast compared with the Mössbauer transition time. Little change was also observed in the Mössbauer spectrum for the LiCl(Fe) system after an isothermal annealing at 200 °C. This shows that the ferrous ions in the LiCl(Fe) sample are stable against the heat treatment at 200 °C.

In the Mössbauer spectrum for the NaCl(Fe) system containing a few at% of iron, three types of absorptions were observed at room temperature (Fig. 12 (b)). They consist of a single line (I_{Na}), one doublet (II_{Na}) with a small quadrupole splitting and the other doublet (III_{Na}) with a large quadrupole splitting (Table 2). According to the X-ray diffraction meas-

urement, a weak shoulder peak was observed on the higher angle side of each diffraction line for the iron-doped sample. This means that this sample has a different phase having a pseudo NaCl structure, in which the lattice constant is somewhat smaller than that of pure NaCl. This fact was justified from the observation of a wavy extinction by means of a polarizing microscopic technique. Therefore, the single line is interpreted as to be caused by the ferrous ions substituted for the sodium ions just as in the case of the lithium chloride system mentioned above. The doublet (III_{Na}) with a large quadrupole splitting is assigned to the aggregate having a pseudo NaCl structure in the host matrix, because its intensity is dependent upon the iron content in the sample. The assignment for the doublet was also justified from the result that there was no absorption of the doublet in the Mössbauer spectrum for NaCl containing about 0.1 at% of enriched iron-57(II) (Fig. 14 (b) and Table 3). The origin of the other doublet (II_{Na}) is not clear. One of the possible explanations for the doublet will be an interstitial site in the sodium chloride sample which has a tetrahedral symmetry.

In the isothermal annealing for the NaCl(Fe) system, the spectral changes took place in the very early stage of the annealing such as 200 °C–1 hr. At first, the outer doublet (III_{Na}) disappeared and a new line due to trivalent iron species was observed. On continuing the annealing, the new line with a large quadrupole splitting ($\delta = 1.21$ mm/sec, $\Delta = 3.01$ mm/sec) grew up at the expense of the original single line (I_{Na}) and the inner doublet (II_{Na}). There is a possibility that this absorption is due to $FeCl_2 \cdot 4H_20$, but it is excluded from the result of a determination of water molecules by means of KARL FISHER's method, *i.e.*, only a trace amount of water was detected. In the light of its large quadrupole splitting and the increased isomer shift value, the new line can be explained by the creation of a new species of divalent iron accompanied by negatively charged vacancy as shown in Fig. 1 (b). Namely, the formation of an iron-vacancy combination will result in a distortion of the cubic symmetry in the environment of the ferrous ions, thus causing an electric field gradient. In addition, the charge density at the iron nucleus will also be changed, because the cation vacancy has an effective negative charge and the electrons around the nucleus will tend to spend more of their time away from the vacancy. Five hour annealing was needed for the complete conversion of the divalent species to the trivalent species. This trivalent species ($\delta = 0.43$ mm/sec) was identified as α-Fe_20_3. X-ray diffraction measurements were also carried out for the sodium chloride system after the different annealing times. The results showed that the shoulder peak mentioned previously disappeared as the annealing proceeded. This is attributed to the decomposition of the aggregate of the metastable pseudo NaCl structure.

The ^{60}Co-γ ray irradiation experiments for LiCl and NaCl samples containing about 0.1 at% of enriched iron-57(II) were also carried out to elucidate the interactions between Fe^{2+} in the crystals and defects as Cl_2^- center formed by irradiations which are reported to be fairly stable in glasses [29, 30].

But there was little change in the Mössbauer parameters before and after γ-ray irradiations as shown in Table 4, which were consistent with the results in ref. 31. This may be due to the fact that Cl_2^- species formed in the crystal such as alkali halide are unstable at room temperature[32].

Table 4. Mössbauer parameters for lithium chloride and sodium chloride samples containing about 0.1 at% of iron-57(II) after γ-ray irradiations. δ, Δ and Γ represent the values of isomer shift, quadrupole splitting and line width, respectively

(mm/sec)

Sample	Dose ($\times 10^8$ R)	δ (± 0.01)	Δ (± 0.02)	Γ (± 0.02)
LiCl (^{57}Fe)	1	1.14	0	0.43
	5	1.14	0	0.45
	10	1.16	0	0.47
NaCl (^{57}Fe)	1	1.15	0	0.32
	5	1.16	0	0.35
	10	1.17	0	0.38

3·2 KCl-$FeCl_2$ and RbCl-$FeCl_2$ systems

In the Mössbauer spectrum for the KCl(Fe) systems containing a few at% of iron, a doublet absorption was observed at room temperature (Fig. 13 (a)), and the value of the isomer shift was characteristic of ferrous ion in the octahedral environment (Table 2). It can be considered that this absorption is due to the ferrous species existing as an aggregate of ferrous chloride in KCl crystal because there was no change in the X-ray diffraction patterns between pure KCl and the iron-doped KCl, and because the ionic radius of K^+ is much larger than that of Fe^{2+}. However, there will also be a possibility of the formation of potassium-chloroferrate compounds ($KFeCl_3$ or K_2FeCl_4), because there was no Mössbauer spectral change after a thermal annealing of the KCl(Fe) sample at 200 °C for 5 hr. Therefore, Mössbauer spectrum measurements for the potassium-chloroferrate compounds prepared in an electric furnace were carried out.

In the Mössbauer spectrum for the sample of K/Fe=1, two types of doublets

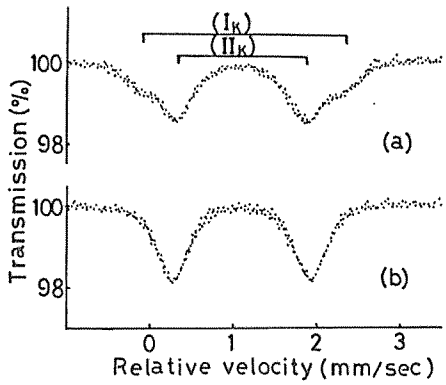

Fig. 15. Mössbauer spectra of KCl-$FeCl_2$ system; (a) K/Fe = 1, (b) K/Fe = 2.

Table 5. Mössbauer parameters for KCl-$FeCl_2$ system. δ and Δ represent the isomer shift and quadrupole splitting values, respectively

(mm/sec)

K/Fe		δ (± 0.01)	Δ (± 0.02)
1	(I_K)	1.16	2.53
	(II_K)	1.15	1.61
2		1.14	1.58
3		1.15	1.62

were observed at room temperature (Fig. 15 (a)). They consist of one doublet (I_K) with a large quadrupole splitting and the other doublet (II_K) with a small quadrupole splitting (Table 5). In the Mössbauer spectrum for the samples of K/Fe=2 and 3, only one doublet (II_K) was observed in every case at room temperature. Only the Mössbauer spectrum for the sample of K/Fe=2 is shown in Fig. 15 (b). All the values of the isomer shift are in the range characteristic of ferrous ion in an octahedral environment (Table 5). The Mössbauer parameters for the absorption (I_K) are consistent with those for the $KFeCl_3$

Table 6. Mössbauer parameters for potassium-chloroferrate compounds. δ and Δ represent the isomer shift and quadrupole splitting values, respectively. After D. H. Leech *et al.*

(mm/sec)

Compound	δ ($\pm$0.01)	Δ ($\pm$0.02)
$KFeCl_3$	1.10	2.37
K_2FeCl_4	1.09 1.07	1.59 1.02

compound reported by D. H. Leech *et al.*[33] (Table 6). In case of sample of K/Fe = 2 or 3, only one doublet absorption (II_K) was observed in our study, while two types of doublets were obtained in the study by D. H. Leech *et al.*[33]. The reason for the two types of doublets was not described in detail in the ref. 33. The difference between our result and theirs may arise from the difference in the preparation method. It is noteworthy that the Mössbauer parameters for the absorption (II_K) are consistent well with those for the outer doublet for the K_2FeCl_4 compound in the ref. 33 (Table 6). Therefore, absorptions (I_K) and (II_K) will be assigned to $KFeCl_3$ and K_2FeCl_4, respectively. These assignments are also confirmed from the X-ray diffraction patterns, *i.e.*, the sample of K/Fe=1 showed two types of lines due to $KFeCl_3$ and K_2FeCl_4, and the samples of K/Fe=2 and 3 showed the lines due to K_2FeCl_4 with a little KCl impurity (Fig. 16).

These results show that K_2FeCl_4 is dominantly formed in the KCl-rich region, which can be understood from the phase diagram of KCl-$FeCl_2$ system by H. L. Pinch *et al.* It seems that the Mössbauer parameters obtained in KCl(Fe) system are consistent with those for K_2FeCl_4 within the experimental error. Therefore,

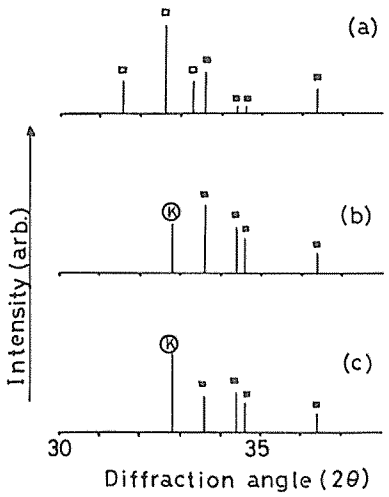

Fig. 16. X-ray diffraction patterns of KCl-$FeCl_2$ system; (a) K/Fe = 1, (b) K/Fe = 2, (c) K/Fe=3. □, ■ and Ⓚ refer to the diffraction lines of $KFeCl_3$, K_2FeCl_4 and KCl, respectively.

it can be considered that the ferrous ion in the KCl crystal exists as K_2FeCl_4 compound when the concentration of the iron is in a few atomic percent. This shows that the K_2FeCl_4 compound is more stable in the KCl-$FeCl_2$ system in comparison with the $KFeCl_3$ compound or the aggregate of the $FeCl_2$ molecules in KCl crystals[34].

In the Mössbauer spectrum for the RbCl(Fe) system containing a few at% of iron, only one doublet absorption was observed at room temperature as in the case of KCl(Fe) system (Fig. 13 (b)). The Mössbauer parameters for this system are somewhat larger than those for KCl(Fe) system (Table 2). Therefore, it is considered that this absorption is due to ferrous species existing as an aggregate of ferrous chloride in the RbCl crystal as in the case of KCl(Fe) system because there was no

change in the X-ray diffraction patterns between pure RbCl and the iron-doped RbCl. However, there will also be a possibility of the formation of rubidium-chloroferrate compounds ($RbFeCl_3$, Rb_2FeCl_4 or Rb_3FeCl_5), because there was no Mössbauer spectral change of the RbCl(Fe) sample after the heat treatment at 200 °C for 5 hr. Therefore, Mössbauer spectrum measurements for rubidium-chloroferrate compounds were also carried out as in the case of KCl(Fe) system.

In the Mössbauer spectrum for the sample of Rb/Fe = 1, two types of doublets were observed at room temperature (Fig. 17 (a)). In the Mössbauer spectrum for the samples of Rb/Fe = 2 and 3, only one doublet was observed in every case at room temperature (Fig. 17 (b)). All the values of the isomer shift are in the range characteristic of ferrous ion (Table 7). The Mössbauer parameters for the inner doublet in the sample of Rb/Fe = 1 are consistent with those (δ = 1.11 mm/sec, Δ = 1.47 mm/sec) for the $RbFeCl_3$ compound reported by P. A. MONTANO *et al.*[35,36]. The Mössbauer parameters for the outer weak doublet absorption in the sample of Rb/Fe = 1 are consistent with

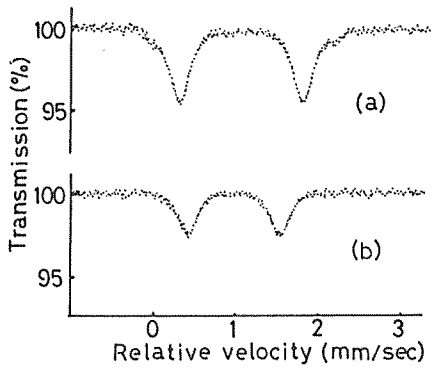

Fig. 17. Mössbauer spectra of RbCl-$FeCl_2$ system; (a) Rb/Fe = 1, (b) Rb/Fe = 2.

Table 7. Mössbauer parameters for RbCl-$FeCl_2$ system. δ and Δ represent the isomer shift and quadrupole splitting values, respectively

(mm/sec)

Rb/Fe	δ (±0.01)	Δ (±0.02)
1	1.08 1.17	1.47 2.32
2	0.95	1.04
3	0.86	1.09

those (δ = 1.12 mm/sec, Δ = 2.29 mm/sec) for $FeCl_2 \cdot 2H_2O$[37,38]. The doublet absorption observed in the samples of Rb/Fe = 2 and 3 will arise from Fe^{2+} in tetrahedral environment, from the value of the Mössbauer parameters (Table 7). This is consistent with the result[24] in the study on the crystalline structure of Rb_3FeCl_5, although the Mössbauer parameters for the Rb_3FeCl_5 compound have not been reported until now. Therefore, the inner and the outer absorption in the sample of Rb/Fe = 1 and the doublet absorption in the samples of Rb/Fe = 2 and 3 will be assigned to $RbFeCl_3$, $FeCl_2 \cdot 2H_2O$ and Rb_3FeCl_5, respectively. These assignments are also confirmed from the X-ray diffraction patterns, *i.e.*, the sample of Rb/Fe = 1 showed the lines due to $RbFeCl_3$ with a little $FeCl_2 \cdot 2H_2O$, and the samples of Rb/Fe = 2 and 3 showed the lines due to Rb_3FeCl_5 with RbCl (Fig. 18). The Rb_2FeCl_4 compound, of which the crystalline structure has not been reported until now, seems not to be formed by the experimental procedures shown in Fig. 11. Therefore, Mössbauer spectrum and X-ray diffraction measurements for the quenched samples of Rb/Fe = 1, 2 and 3 were carried out for comparison.

In all the Mössbauer spectra for the quenched samples of Rb/Fe = 1, 2 and 3, three types of absorptions were observed

in contrast with the case of the slowly cooled samples mentioned previously, while there was no change in the Mössbauer spectrum between slowly cooled and quenched samples of K/Fe = 1, 2 and 3. They consist of the absorption (I_{Rb}) due to the $RbFeCl_3$ compound, the absorption (III_{Rb}) due to the Rb_3FeCl_5 compound and a new doublet absorption (II_{Rb}) with a larger quadrupole splitting (Figs. 19 (a) and 20 (a)). The isomer shift value for the new absorption (II_{Rb}) falls in the range characteristic of ferrous ion in octahedral environments (Tables 8 and 9).

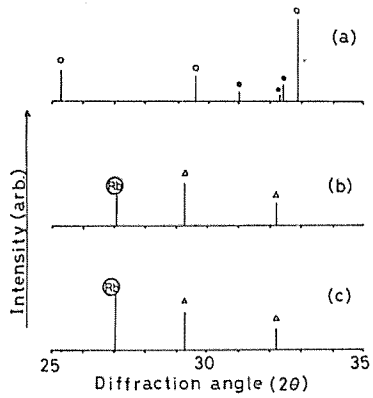

Fig. 18. X-ray diffraction patterns of RbCl-$FeCl_2$ system; (a) Rb/Fe = 1, (b) Rb/Fe = 2, (c) Rb/Fe = 3. ○, △, ● and (Rb) refer to the diffraction lines of $RbFeCl_3$, Rb_3FeCl_5, $FeCl_2 \cdot 2H_2O$ and RbCl, respectively.

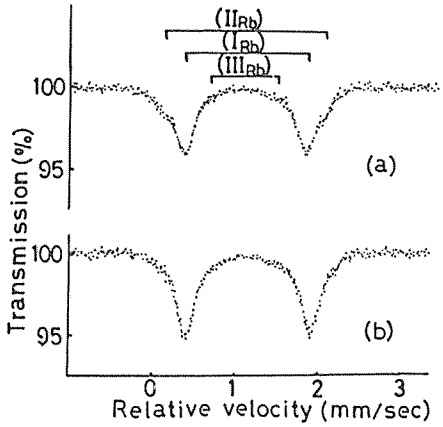

Fig. 19. Mössbauer spectra of the quenched sample of Rb/Fe = 1 before (a) and after (b) the heat treatment at 300°C for 5 hr under H_2 atmosphere.

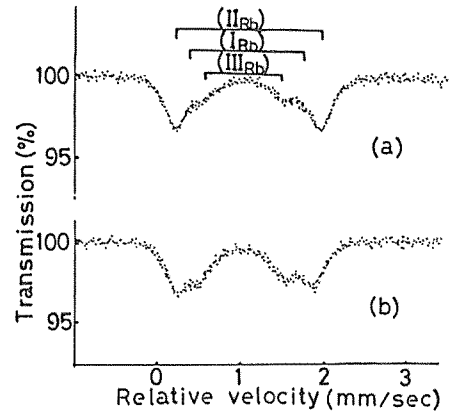

Fig. 20. Mössbauer spectra of the quenched sample of Rb/Fe = 2 before (a) and after (b) the heat treatment at 300°C for 5 hr under H_2 atmosphere.

Table. 8. Mössbauer parameters for the quenched sample of Rb/Fe = 1 before and after the heat treatment. δ and Δ represent the isomer shift and quadrupole splitting values, respectively

(mm/sec)

Sample		δ (±0.01)	Δ (±0.02)	S (%)*
Quenched	(I_{Rb})	1.14	1.39	70
	(II_{Rb})	1.15	1.71	21
	(III_{Rb})	1.07	0.99	9
Heated (300 °C − 5 hr)	(I_{Rb})	1.12	1.43	80
	(II_{Rb})	1.18	1.73	11
	(III_{Rb})	1.05	1.01	9

* the ratio of peak area.

Table 9. Mössbauer parameters for the quenched sample of Rb/Fe = 2 before and after the heat treatment. δ and Δ represent the isomer shift and quadrupole splitting values, respectively

(mm/sec)

Sample		δ (±0.01)	Δ (±0.02)	S(%)*
Quenched	(I_{Rb})	1.14	1.40	10
	(II_{Rb})	1.17	1.71	76
	(III_{Rb})	1.10	1.15	14
Heated (300 °C −5 hr)	(I_{Rb})	1.15	1.42	8
	(II_{Rb})	1.18	1.70	63
	(III_{Rb})	1.08	0.99	29

* the ratio of peak area.

In the Mössbauer spectrum of the quenched sample of Rb/Fe = 1 after the heat treatment at 300°C for 5 hr under H_2 atmosphere, the increase of absorption (I_{Rb}) due to the $RbFeCl_3$ compound was observed with the decrease of the new doublet absorption (II_{Rb}) (Fig. 19 (b) and Table 8). In the Mössbauer spectrum of the quenched sample of Rb/Fe = 2 after the heat treatment at 300°C for 5hr under H_2 atmosphere, the increase of absorption (III_{Rb}) due to the Rb_3FeCl_5 compound was observed with the decrease of the new doublet absorption (II_{Rb}) (Fig. 20 (b) and Table9). In X-ray diffraction patterns for the quenched sample of Rb/Fe = 1 after the heat treatment, the increase of the intensity of diffraction lines due to the $RbFeCl_3$ compound was observed with the decrease of that of the new diffraction lines, and for the quenched sample of Rb/Fe = 2 after the heat treatment, the increase of the intensity of diffraction lines due to the Rb_3FeCl_5 compound was also observed with the decrease of that of the new diffraction lines just as in the case of the Mössbauer spectral change (Figs. 21 and 22). Therefore, provided that the new diffraction lines should be due to the Rb_2FeCl_4 compound of which the crystalline structure is unknown, these findings described above will support the conception that the following reactions have taken place during the heat treatment.

$Rb_2FeCl_4 \rightarrow RbFeCl_3 + RbCl$ for the quenched sample of Rb/Fe = 1

and

$Rb_2FeCl_4 + RbCl \rightarrow Rb_3FeCl_5$ for the quenched sample of Rb/Fe=2.

It is noteworthy that the Mössbauer parameters for the RbCl(Fe) containing a few at% of iron are consistent with those

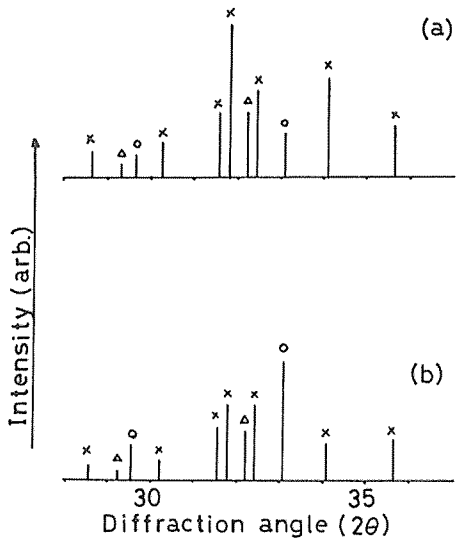

Fig. 21. X-ray diffraction patterns of the quenched sample of Rb/Fe = 1 before (a) and after (b) the heat treatment at 300°C for 5hr under H_2 atmosphere. ○ and △ refer to the diffraction lines of $RbFeCl_3$ and Rb_3FeCl_5, respectively. × also refers to the new diffraction lines.

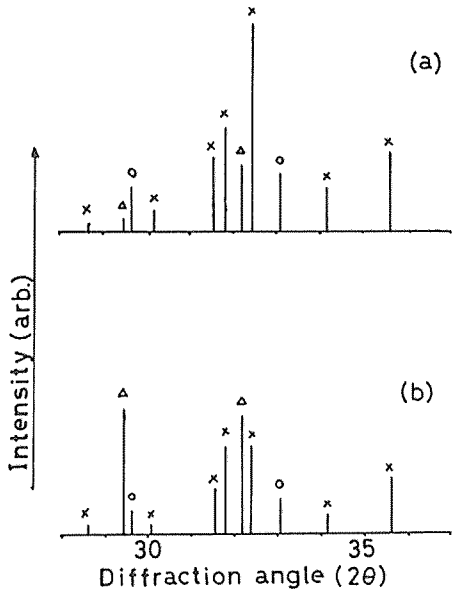

Fig. 22. X-ray diffraction patterns of the quenched sample of Rb/Fe = 2 before (a) and after (b) the heat treatment at 300°C for 5hr under H_2 atmosphere. ○ and △ refer to the diffraction lines of $RbFeCl_3$ and Rb_3FeCl_5, respectively. × also refers to the new diffraction lines.

for the Rb_2FeCl_4 compound described above within the experimental error. Therefore, it can be considered that the ferrous ion in the RbCl crystal also exists as Rb_2FeCl_4 compound when the concentration of the iron is in a few at%, because the Rb_2FeCl_4 compound is formed only for the quenched system. This shows that the Rb_2FeCl_4 compound is unstable from the thermodynamical point of view as described above, but that it is more stable in RbCl(Fe) system in comparison with the aggregate of $FeCl_2$ molecules in RbCl crystals.

The ^{60}Co-γ ray irradiation experiments were also carried out for the potassium- and rubidium-chloroferrate compounds, but γ-ray irradiation effects were not observed (Table 10). This shows that the chloroferrate(II) ion in these ionic compounds is fairly stable against γ-rays.

Table 10. Mössbauer parameters for the potassium- and rubidium-chloroferrate compounds after γ-ray irradiations. δ, Δ and Γ represent the values of isomer shift, quadrupole splitting and the line width, respectively

(mm/sec)

Compound	Dose ($\times 10^6$ R)	δ (±0.01)	Δ (±0.02)	Γ (±0.02)
$KFeCl_3$	1	1.17	2.52	0.53
	5	1.19	2.54	0.51
	10	1.20	2.56	0.52
K_2FeCl_4	1	1.15	1.59	0.45
	5	1.16	1.61	0.46
	10	1.18	1.63	0.44
$RbFeCl_3$	1	1.11	1.44	0.30
	5	1.13	1.46	0.31
	10	1.14	1.49	0.32
Rb_2FeCl_4	1	1.16	1.72	0.31
	5	1.18	1.73	0.30
	10	1.20	1.75	0.29
Rb_3FeCl_5	1	1.00	1.03	0.28
	5	1.03	1.05	0.29
	10	1.04	1.07	0.30

3·3 CsCl-$FeCl_2$ system

The Mössbauer spectrum for the CsCl(Fe) system containing a few at% of iron was not observed at room temperature, and so the spectrum measurement was carried out at liquid nitrogen temperature. In the spectrum, only one doublet absorption was observed (Fig. 13 (c)). The value of isomer shift falls in the range characteristic of ionic ferrous ion. In X-ray diffraction patterns for the CsCl(Fe) system, new complex patterns were observed

with a little CsCl. It was found that the new patterns are consistent with the diffraction patterns due to the Cs_3FeCl_5 compound. Therefore, the doublet absorption will be due to Cs_3FeCl_5. This assignment is justified from the fact that the Mössbauer parameters for the doublet are consistent with those for Cs_3FeCl_5 in ref. 33.

Therefore, it will be considered that the ferrous ion in the CsCl crystal exists as the Cs_3FeCl_5 compound when the concentration of the iron is in a few at%, just as in the cases of KCl-$FeCl_2$ and RbCl-$FeCl_2$ systems.

References

1) F. SEITZ: *Revs. Modern Phys.*, **26**, 11 (1954).
2) J. R. REITZ and J. L. GAMMEL: *J. Chem. Phys.*, **19**, 894 (1951).
3) F. BASSANI and F. G. FUMI: *Nuovo cimento*, **11**, 274 (1954).
4) M. P. TOSI and G. AIROLDI: *Nuovo cimento*, 8, 584 (1958).
5) CAMAGNI, CHIAROTTI, FUMI and GIULOTTO: *Phil. Mag.*, **45**, 225 (1954).
6) F. REIF: *Phys. Rev.*, **100**, 1597 (1955).
7) N. N. GREENWOOD: *Angew. Chem. Internal. Edit.*, **10**, 716 (1971).
8) J. M. FRIEDT and J. DANON: *Radiochim. Acta*, **17**, 173 (1972).
9) G. VOGL: *J. Physique*, **35**, C6-165 (1974).
10) J. G. MULLEN: *Phys. Rev.*, **131**, 1410 (1963).
11) J. G. MULLEN: *Phys. Rev.*, **131**, 1415 (1963).
12) K. HENNIG and Kim YUNG: *Phys. Stat. Sol.*, **40**, 365 (1970).
13) R. CAPPELETTI, R. FIESCHI and C. LAMBORIZIO: *Radiat. Eff.*, 4, 95 (1970).
14) A. N. MURIN, B. G. LURE and P. O. SEREGIN: *Fiz. tverd. Tela*, **9**, 1424 (1967): *Soviet Phys.—solid state*, **9**, 1110 (1967).
15) R. KAMAL and R. G. MENDIRATTA: *Phys. Rev., B*, **7**, 80 (1973).
16) M. DECOSTER and S. AMELINCKX: *Phys. Lett.*, **1**, 245 (1962).
17) A. G. MADDOCK, A. F. WILLIAMS, K. E. SIEKIERSKA and J. FENGER: *Phys. Stat. Sol. (b)*, **74**, 183 (1976).
18) S. M. EDELGLASS and M.OHRING: *Phys. Stat. Sol. (a)*, **17**, 567 (1973).
19) G. K. WERTHEIM and H. J. GUGGENHEIM: *J. Chem. Phys.*, **42**, 3873 (1965).
20) A. N. MURIN and P. P. SEREGIN: *Phys. Stat. Sol. (a)*, **2**, 663 (1970).
21) G. D. WATKINS: *Phys. Rev.*, **113**, 79 (1959).
22) N. KAI, T. NISHIDA and Y. TAKASHIMA: *Radiochem. Radioanal. Lett.*, **44**, 181 (1980).
23) H. L. PINCH and J. M. HIRSHON: J. *Am. Chem. Soc.*, **79**, 6149 (1957).
24) H. J. SEIFERT and K. KLATYK: *Z. Anorg. Allg. Chem.*, **342**, 1 (1966).
25) G. M. BANCROFT, M. J. MAYS and B. E. PRATER: *Chem. Phys. Lett.*, **4**, 248 (1969).
26) L. ASCH, J. P. ADLOFF, J. M. FRIEDT and J. DANON: *Chem. Phys. Lett.*, **5**, 105 (1970).
27) J. STEGER and E. KOSTINER: *J. Chem. Phys.*, **58**, 3389 (1973).
28) Y. TAKASHIMA, N. KAI, T. NISHIDA and L. CHANDLER: *J. Physique*, **40**, C2-566 (1979).
29) D. L. GRISCOM, P. C. TAYLOR and P. J. BRAY: *J. Chem. Phys.*, **50**, 977 (1969).
30) T. NISHIDA, N. KAI and Y. TAKASHIMA: *Phys. Chem. Glasses*, to be published.
31) Y. TAKASHIMA, N. KAI, T. NISHIDA and Y. NAKAYAMA: *Memoirs of the*

Faculty of Science, Kyushu University Ser. C, **12**, 149 (1980).
32) T. G. CASTNER and W. KÄNZIC: *J. Phys. Chem. Solids*, **3**, 178 (1957).
33) D. H. LEECH and D. J. MACHIN: *J. Inorg. Nucl. Chem.*, **37**, 2279 (1975).
34) Y. TAKASHIMA, N. KAI and T. NISHIDA: *Radiochem. Radioanal. Lett.*, **43**, 287 (1980).
35) P. A. MONTANO, E. COHEN, H. SHECHTER and J. MAKOVSKY: *Phys. Rev. B*, **7**, 1180 (1973).
36) P. A. MONTANO, H. SHECHTER, E. COHEN and J. MAKOVSKY: *Phys. Rev. B*, **9**, 1066 (1974).
37) C. E. JOHNSON: *Proc. Phys. Soc.*, 88, 943 (1966).
38) C. D. BURBRIDGE and D. M. L. GOODGAME: *J. Chem. Soc. (A)*, 1410 (1968).

Acknowledgements

The author is very grateful to Professor Yoshimasa TAKASHIMA of Kyushu University for his helpful and constructive comments on the manuscript, and for his continuous encouragement throughout the study.

The author is also very grateful to Professor Shigeru OHASHI and Assistant Professor Hirohiko WAKI of Kyushu University for their helpful and constructive comments on the manuscript.

The author is also very grateful to Dr. Tetsuaki NISHIDA of Kyushu University for his helpful comments on the manuscript.

The author is very grateful to Dr. Yonezo MAEDA, Dr. Susumu OSAKI and Mr. Noriyuki MOMOSHIMA of Kyushu University for their helpful discussions throughout the study.

微量の鉄(II)を含むアルカリ塩化物結晶のメスバウァー分光学的研究

甲斐　徳久

微量の ^{57}Co をドープしたアルカリハライド結晶の発光メスバウァースペクトルは，現在までいくつか報告されている。しかしながら，得られた吸収についての考察は様々で，中には相反しているものもみられる。これは ^{57}Co の EC 壊変に伴う後遺効果についての解釈が様々であることによると考えられる。そこで，本研究では，吸収メスバウァー分光法を用いてアルカリ塩化物結晶中の微量の Fe^{2+} の挙動について考察した。その結果，アルカリ塩化物結晶中の Fe^{2+} は，そのイオン半径とくらべてイオン半径のあまりかわらないアルカリ金属イオン（Li^+ 及び Na^+）とは完全に置換して存在し，イオン半径のきわめて大きなアルカリ金属イオン（K^+，Rb^+ 及び Cs^+）とは置換して存在するというよりはむしろ結晶内でそれぞれの化合物（K_2FeCl_4，Rb_2FeCl_4 及び Cs_3FeCl_5）として安定に存在すると結論された。